



THE UNIVERSITY *of* EDINBURGH

Edinburgh Research Explorer

A flow-system array for the discovery and scale up of inorganic clusters

Citation for published version:

Richmond, CJ, Miras, HN, de la Oliva, AR, Zang, H, Sans, V, Paramonov, L, Makatsoris, C, Inglis, R, Brechin, EK, Long, D-L & Cronin, L 2012, 'A flow-system array for the discovery and scale up of inorganic clusters' Nature Chemistry, vol 4, no. 12, pp. 1037-1043. DOI: 10.1038/NCHEM.1489

Digital Object Identifier (DOI):

[10.1038/NCHEM.1489](https://doi.org/10.1038/NCHEM.1489)

Link:

[Link to publication record in Edinburgh Research Explorer](#)

Document Version:

Peer reviewed version

Published In:

Nature Chemistry

Publisher Rights Statement:

Copyright © 2012 Macmillan Publishers Limited. All rights reserved.

General rights

Copyright for the publications made accessible via the Edinburgh Research Explorer is retained by the author(s) and / or other copyright owners and it is a condition of accessing these publications that users recognise and abide by the legal requirements associated with these rights.

Take down policy

The University of Edinburgh has made every reasonable effort to ensure that Edinburgh Research Explorer content complies with UK legislation. If you believe that the public display of this file breaches copyright please contact openaccess@ed.ac.uk providing details, and we will remove access to the work immediately and investigate your claim.



Post-print of peer-reviewed article published by the Nature Publishing Group.

Published article available at: <http://dx.doi.org/10.1038/nchem.1489>

Cite as:

Richmond, C. J., Miras, H. N., de la Oliva, A. R., Zang, H., Sans, V., Paramonov, L., Makatsoris, C., Inglis, R., Brechin, E. K., Long, D-L., & Cronin, L. (2012). A flow-system array for the discovery and scale up of inorganic clusters. *Nature Chemistry*, 4(12), 1037-1043.

Manuscript received: 06/02/2012; Accepted: 28/09/2012; Article published: 18/11/2012

A flow-system array for the discovery and scale up of inorganic clusters**

Craig J. Richmond,¹ Haralampos N. Miras,¹ Andreu Ruiz de la Oliva,¹ Hongying Zang,¹ Victor Sans,¹
Leonid Paramonov,² Charalampos Makatsoris,² Ross Inglis,³ Euan K. Brechin,³ De-Liang Long¹
and Leroy Cronin^{1,*}

^[1]WestCHEM, School of Chemistry, University of Glasgow, University Avenue, Glasgow G12 8QQ, UK.

^[2]School of Engineering and Design, Brunel University, Uxbridge, Middlesex UB8 3PH, UK.

^[3]EaStCHEM, School of Chemistry, Joseph Black Building, University of Edinburgh, West Mains Road, Edinburgh, EH9 3JJ, UK.

^[*]Corresponding author; e-mail: Lee.Cronin@glasgow.ac.uk

^[**]This work was supported by the EPSRC, WestCHEM, The Leverhulme Trust, and the University of Glasgow.

Supporting information:

Supplementary Information accompanies the paper on www.nature.com/nchem

Author Contributions:

C.J.R. and L.C. designed experiments analyzed data, prepared the figures and wrote the manuscript. H.N.M. provided invaluable advice and assisted with crystallography. A.R. corroborated the syntheses and compound analysis. D.L. solved and checked the crystallographic data. L.P. and C.M. wrote the software interface used for the programmed pump control. E.K.B and R.I provided help with the synthesis of the Mn-based complexes.

Abstract

The ‘one-pot’ batch discovery of complex nanoscale and supermolecular systems is a fantastic challenge since although the process of discovery can yield amazing results, repeatability and scale-up are significant challenges that have acted as a road block to further application and development. In organic synthesis the move from batch to flow processing has dramatically increased the efficiency of many organic synthetic procedures but the syntheses of many supermolecular and supramolecular inorganic cluster compounds, such as polyoxometalates (POMs) and single molecule magnets (SMMs), still rely heavily upon time consuming ‘one-pot’ batch processing and crystallization and could therefore also benefit from such a switch to more continuous or autonomous synthetic methods. To explore this we have combined an automated flow process with multiple batch crystallizations to create a highly efficient method for both screening and scaling-up the syntheses of exemplary compounds of this nature: Firstly the custom built autonomous reactor system was used to synthesise well-known polyoxomolybdate clusters, including the $\{\text{Mo}_{154}\}$ “molybdenum blue wheel” and the $\{\text{Mo}_{368}\}$ “giant molybdenum lemon”. The scope of the synthetic approach was then extended to include a family of well-studied Mn Single Molecule Magnets. Synthesis of these architectures was achieved by programming the multiple pump reactor system to sequentially vary the relative flow rates of the reagent solutions, thus exploring a large section of parameter space in a much shorter time period than conventional batch procedures. From the array of reactions produced, successful conditions for product isolation could be easily identified and a direct route to “scale-up” was then immediately available simply by continuous application of those flow conditions. This allowed the reliable scale-up of complex molecular syntheses, leading to gram quantities of phase pure material whilst also decreasing the time taken for the discovery, repetition and scale-up processes.

Introduction

The benefits of continuous flow processing in synthetic organic chemistry have been well researched and documented in recent years.^[1] Key advantages include higher efficiencies of heat transfer and rapid homogeneous mixing, leading to increased reaction rates, yields and selectivities.^[2] Continuous flow process techniques have also proved useful in inorganic synthesis, however examples are limited mainly to the production of metallic and semiconductor nanoparticles and quantum dots.^[3] Other major areas of interest in inorganic chemistry, such as polyoxometalates (POMs)^[4] and Single Molecule Magnets (SMMs),^[5] typically utilize batch syntheses and purification *via* crystallization. Screening of reaction conditions for the discovery of novel architectures must therefore cover a large area of synthetic space as it not only has to achieve conditions suitable for the target formation but target crystallization as well. Large number reaction arrays are therefore an inherent aspect in the

discovery process, which can be an extremely laborious and time consuming task when working solely under batch conditions.

Herein the combination of autonomous flow processing with multiple batch crystallization is presented as a new efficient method capable of both the rapid construction of large number reaction arrays for molecular discovery and the continuous generation of batch reactions required during scale-up. As an initial proof of concept the multiple pump reactor setup was applied in the production of a selection of polyoxomolybdates of various sizes and structural complexity; **1**, $\text{Na}_8[\text{Mo}_{36}\text{O}_{112}(\text{H}_2\text{O})_{16}] \cdot 58\text{H}_2\text{O} = \{\text{Mo}_{36}\}$; **2**, $\text{Na}_{15}[\text{Mo}^{\text{VI}}_{126}\text{Mo}^{\text{V}}_{28}\text{O}_{462}\text{H}_{14}(\text{H}_2\text{O})_{70}]_{0.5} [\text{Mo}^{\text{VI}}_{124}\text{Mo}^{\text{V}}_{28}\text{O}_{457}\text{H}_{14}(\text{H}_2\text{O})_{68}]_{0.5} \cdot \text{ca. } 400 \text{ H}_2\text{O} = \{\text{Mo}_{154}\}$; **3**, $(\text{NH}_4)_{42}[\text{Mo}^{\text{VI}}_{72}\text{Mo}^{\text{V}}_{60}\text{O}_{372}(\text{CH}_3\text{COO})_{30}(\text{H}_2\text{O})_{72}] \cdot \text{ca. } 300 \text{ H}_2\text{O} \cdot \text{ca. } 10\text{CH}_3\text{COONH}_4 = \{\text{Mo}_{132}\}$; **4**, $\text{Na}_{12}[\text{Mo}^{\text{VI}}_{72}\text{Mo}^{\text{V}}_{30}\text{O}_{282}(\text{SO}_4)_{12}(\text{H}_2\text{O})_{78}] \cdot \text{ca. } 280 \text{ H}_2\text{O} = \{\text{Mo}_{102}\}$; and **5**, $\text{Na}_{48}[\text{H}_x\text{Mo}_{368}\text{O}_{1032}(\text{H}_2\text{O})_{240}(\text{SO}_4)_{48}] \cdot \text{ca. } 1000\text{H}_2\text{O} = \{\text{Mo}_{368}\}$.^[6] To further demonstrate the scope of this method, the syntheses of a number of coordination clusters with single molecular magnetic (SMM) properties were also explored; **6**, $\text{Mn}_3\text{O}(\text{Et-sao})_3(\text{MeOH})_3(\text{ClO}_4)$; **7**, $\text{Mn}_3\text{O}(\text{Et-sao})_3(\text{tBuPy})_3(\text{ClO}_4)$; **8**, $\text{Mn}_5\text{O}_2(\text{Et-sao})_6(\text{MeO})(\text{H}_2\text{O})(\text{MeOH})_2$; and **9**, $\text{Mn}_6\text{O}_2(\text{Et-sao})_6(\text{Piv})_2(\text{MeOH})_6$.^[7] The setup utilized eight programmable syringe pumps (C3000 model, Tricontinent Ltd, CA, USA), although this is extendable to fifteen, and a LabVIEW™ based PC interface for controlling the pumps (Figure 1).

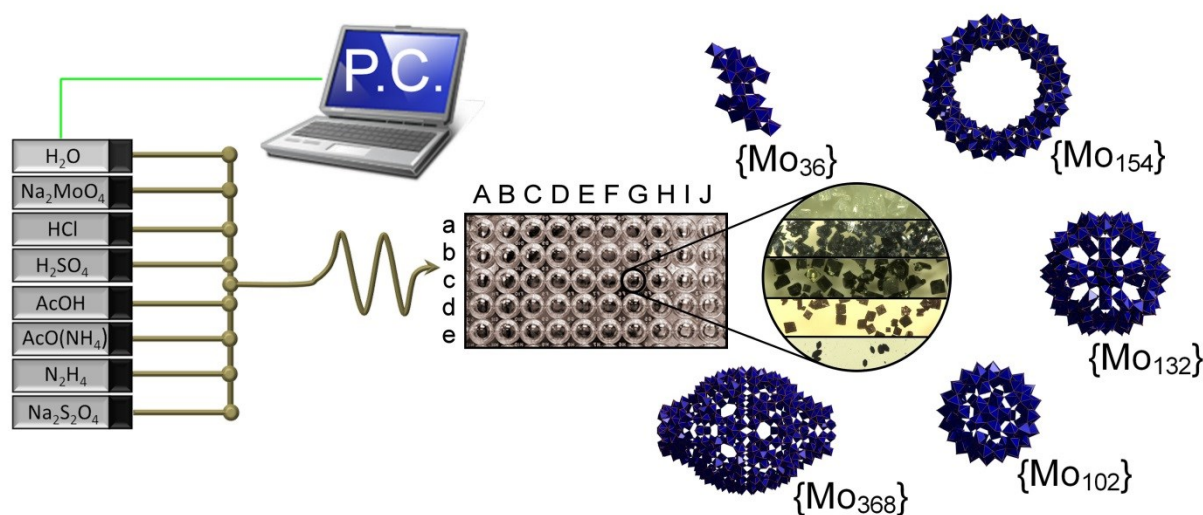


Figure 1. Schematic of the pump setup showing reactor tubing connectivity and computer aided control (left). Representative image of the 5×10 reaction array outputs produced during the discovery experiment runs (middle). Images of the crystal batches and polyhedral representations for the target polyoxomolybdates obtained; $\{\text{Mo}_{36}\}$, $\{\text{Mo}_{154}\}$, $\{\text{Mo}_{132}\}$, $\{\text{Mo}_{102}\}$ and $\{\text{Mo}_{368}\}$ (right).

The reagent set chosen for POM synthesis consisted of distilled deionized water for dilution, 2.5 M $\text{Na}_2\text{MoO}_4 \cdot 2 \text{H}_2\text{O}$ as the molybdenum source, three acid sources 5.0 M HCl, 1.0 M H_2SO_4 , and 50% AcOH, 4.0 M $\text{AcO}(\text{NH}_4)$, and two sources of reducing agent, 0.25 M $\text{Na}_2\text{S}_2\text{O}_4$ and saturated (0.23M) $\text{N}_2\text{H}_2 \cdot \text{H}_2\text{SO}_4$. For the simplest POM target compound, **1** $\{\text{Mo}_{36}\}$, only three of the eight pumps were required to incrementally vary the relative flow rates of the water, molybdate and HCl stock solutions, for compounds **2** $\{\text{Mo}_{154}\}$, **3** $\{\text{Mo}_{132}\}$, **4** $\{\text{Mo}_{102}\}$, and **5** $\{\text{Mo}_{368}\}$ up to five pumps were required to supply the additional reducing agent and buffer stocks.

Ratios of Water Flow Rates to Reagent Flow Rates		Ratios of Acid Flow Rates to Molybdenum Flow Rates									
		0:10	1:9	2:8	3:7	4:6	5:5	6:4	7:3	8:2	9:1
		A	B	C	D	E	F	G	H	I	J
8:2	a										
6:4	b										
4:6	c										
2:8	d										
0:10	e										

Figure 2. Table depicting arbitrary flow rates for the reagents used to create the 5×10 reaction discovery arrays. Down columns A-J the dilution factor decreases, dictated by the ratio of the flow rates for the water pump versus all other reagents, indicated by the dimpled shading. Across rows a-e the ratios of the pump rates for the acid (or buffer) versus molybdate increase, indicated by the colour gradient. One programmed reaction run therefore automatically scans 50 reactions, ranging from high to low pH and low to high reagent concentration.

The first reported synthesis of the $\{\text{Mo}_{36}\}$ structure by Krebs simply acidified an aqueous solution of sodium molybdate which subsequently precipitated crystals of the target compound.^[6a] However, as with most syntheses only the best synthetic conditions are reported and the arduous work that went into finding them is glossed over, when even mentioned at all. Therefore our focus was to prepare a simple pump setup that could repeat this screening process but with minimal human input. With $\{\text{Mo}_{36}\}$ in mind as a primary target for our “discovery array” the pumps were programmed to run at a range of flow rates, incrementally increasing both the relative ratio of acid to molybdate and the overall reagent concentrations, two key parameters of POM formation and crystallization, throughout the experiment run. As shown in figure 2, the volume of acid with respect to Mo was varied from 0% to 90% (across rows) and the volume of additional water with respect to the total reagent volume was varied from 80% to 0% (down columns). Independent variation of just these two parameters resulted

in the output of fifty distinct reaction conditions that could have potentially led to the formation of the $\{Mo_{36}\}$ target. The combined flow rate for all pumps running at any specific point was set to 12.5 mL min^{-1} in order to maintain a consistent output flow velocity and reaction volume, the variation of the output flow composition was controlled by varying the rates of the individual pumps relative to one another. A length of tubing (6.22 m) of relatively wide bore (1.6 mm ID) was placed after the mixing manifold to allow dissolution of transient precipitates that are typically observed upon acidification of molybdate salts. The diameter was chosen to be sufficiently wide enough to avoid blockage of the system upon formation of such precipitates and the tubing length was chosen to coincide with the reaction volumes collected: The relative flow rates were changed every 30 sec thus giving a reaction volume of 6.25 mL (*i.e.* $\frac{1}{2} \text{ min} \times 12.5 \text{ mL min}^{-1}$) for each reaction composition and the total volume for the tubing was 12.5 mL (*i.e.* $2 \times$ reaction volumes or 1 min residence time). The individual reaction mixtures were collected every 30 sec with a 1.5 sec delay to allow for changing of the test tubes during collection. An entire run of fifty reactions, scanning conditions from high to low dilution and high to low pH therefore took less than 35 min to complete. As confirmation of the reaction mixture compositions matching the theoretical values from the programmed flow rates, the pH of the individual reactions within the “discovery array” was measured immediately after collection (Figure 3a.). The pH can be seen to fluctuate from high to low periodically across the array of reactions, which maps directly to the conditions imposed by the pre-programmed screening sequence (Figure 1.): Reaction number 1 (or aA) contains no acid and the dilution factor is 8:2 therefore 80% of the reaction volume comes purely from the water stock and the remaining 20% from the 2.5 M $Na_2MoO_4 \cdot 2H_2O$ stock, a relatively high pH of *ca.* 6-7 is consistent with a solution of this composition. From reactions 2-10 (or aB – aJ) the overall trend is a gradual decrease in pH as the acid content increases with respect to the Mo, with the dilution factor remaining constant at 8:2. For reaction number 11 (bA) the pH jumps back up as the flow rates revert back to 0% acid, however now at a slightly higher Mo concentration due to the decreased dilution factor of 6:4. This trend is repeated across the remainder of the array as the acid: Mo ratio and dilution factor vary as dictated by the pre-programmed screening sequence.

(turn to next page →)

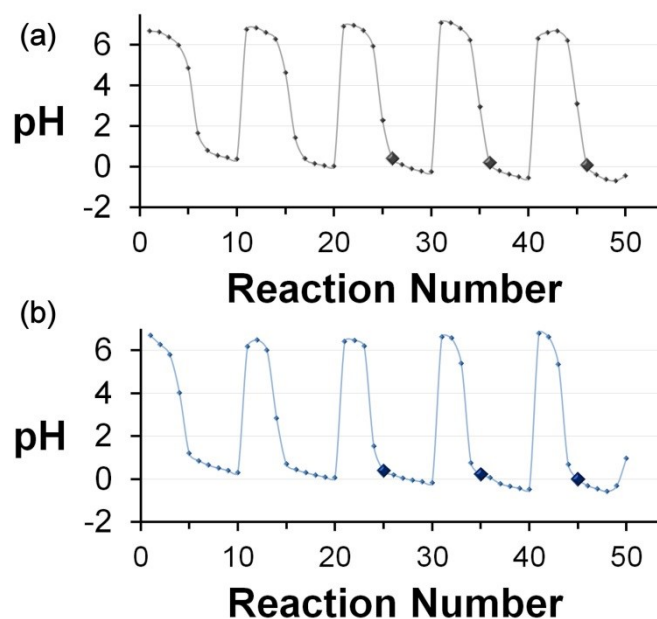
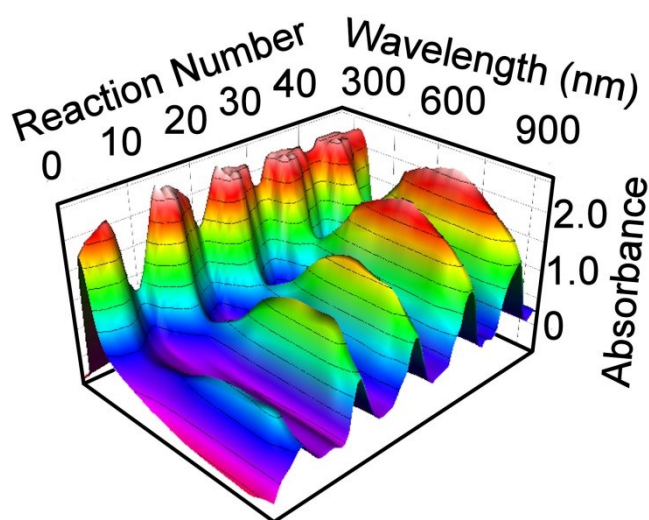


Figure 3. Charts of pH measurements for the 5×10 discovery array experiments for; (a) $\{\text{Mo}_{36}\}$ synthesis and (b) $\{\text{Mo}_{154}\}$ synthesis. The pH varies periodically in all cases as the ratios of the flow rates for the acids / molybdate increase for each dilution factor. Data points for reactions resulting in successful crystallization are highlighted. The reaction number corresponds to fractions being collected sequentially as 5 rows of 10 in the 50 reaction array (*i.e.* 1 -10 is aA – aJ, 11 – 20 is bA – bJ, 21 – 30 is cA – cJ, 31 – 40 is dA – dJ, 41 – 50 is eA – eJ).

After leaving the solutions undisturbed in open air for 24 hours three out of the fifty reactions had precipitated colourless columnar crystals, reaction numbers 26 (cF), 36 (dF) and 46 (eF). Single crystal X-ray diffraction and IR spectroscopy were used to confirm the crystalline product as pure $\{\text{Mo}_{36}\}$. Note that these conditions have low pH and high Mo concentration, which coincides with the traditional batch synthesis.^[6a] The remaining reaction solutions had either remained as colourless solutions or had precipitated an amorphous white powder. For those reactions that had remained colourless solutions, an attempt was made to identify the condensed molybdate species in solution from Dynamic Light Scattering (DLS) measurements taken of the reaction solutions (see supplementary fig. S3). Particle sizes of 1.7-2 nm were consistently observed for the more dilute solutions at low pH, indicating formation of a condensed molybdenum species of similar size to $\{\text{Mo}_{36}\}$. Indeed, after leaving some of these solutions for a few more days, a handful of colourless columnar crystals formed which were also confirmed to be $\{\text{Mo}_{36}\}$ (unit cell match).

The next target structure for the discovery array setup was the reduced “molybdenum blue wheel”, $2 \{\text{Mo}_{154}\}$, first characterized by Müller *et. al.*,^[8] and produced in batch *via* the partial reduction of an acidified molybdate solution with a reducing agent such as sodium dithionite. An additional pump

containing a solution of 0.25 M $\text{Na}_2\text{S}_2\text{O}_4$ was therefore programmed to provide 10 mol% reducing agent with respect to Mo during scanning of the reaction parameters, where again the relative reagent ratios and levels of dilutions throughout were incrementally altered over the experiment run. The dithionite pump flow rate was set to scale directly with the molybdate pump flow rate thus giving a constant reduction environment for all fifty reactions. The reducing agent pump flow rate could have been set as a new variable parameter however it is well known that increasing this value beyond 10 mol% results in increased levels of amorphous polymeric molybdenum oxide species^[6b] and so would have increased the array dimensions without increasing the potential to isolate high quality crystalline products suitable for structure determination. A similar pattern in the pH values measured for the $\{\text{Mo}_{154}\}$ discovery array was observed; as expected the pH fluctuated across the array as the acid content and dilution ratios varied in accordance with the preprogrammed reagent flow rates (Figure 3b). The fifty reactions from the array were again left undisturbed for 24 hours before checking for successful crystallization. Again three out of the fifty reactions precipitated crystalline material, reaction numbers 26 (cF), 35 (dE) and 45 (eE), the remaining reactions either precipitated no material or precipitated a dark amorphous material not suitable for crystallographic analysis. As before, the low pH and high Mo concentrations for successful product isolation were consistent with the original batch conditions and the crystalline products confirmed as $\{\text{Mo}_{154}\}$ by unit cell checks, IR and absorbance spectroscopy.^[6b] In addition to pH measurements, absorbance spectroscopy was also used to monitor the change in the reaction composition across the reaction array. Figure 4 shows a 3D plot of the absorbance spectra for the 5×10 reaction array. The absorbance at ~ 750 nm (indicative of Mo-blue species)^[6b] was observed to coincide with the periodic fluctuations in pH, again demonstrating that the resulting reaction conditions were consistent with the preprogrammed flow rates.



← **Figure 4.** Plot of diluted fractions of the $\{\text{Mo}_{154}\}$ reaction array showing a similar periodic trend to pH. Reaction number corresponds to fractions being collected sequentially as 5 rows of 10 in the 50 reaction array (*i.e.* 1 -10 is aA – aJ, 11 – 20 is bA – bJ, 21 – 30 is cA – cJ, 31 – 40 is dA – dJ, 41 – 50 is eA – eJ). Samples diluted 1:16 with distilled water and filtered before absorbance measurements.

Next, compound **3**, the $\{\text{Mo}_{132}\}$ Keplerate^[6c] spherical cluster was then targeted, which required the operation of the AcOH and AcO(NH₄) reagent pumps in place of the HCl pump and N₂H₂·H₂SO₄ in place of Na₂S₂O₄. The ratio of (NH₄)OAc to AcOH flow rates was set to 1:1 to provide a buffered solution of *ca.* pH 4. The discovery array experiment was then run as before, altering the ratio of reduced molybdenum : buffer reagents in addition to the level of dilution. The level of reduction was set at 20 mol% in accordance with the approximate ratio of Mo^V : Mo^{VI} in the $\{\text{Mo}_{132}\}$ target. The pH of the reactions within the array again varied periodically (see supplementary fig. S2) however over the narrower pH range of *ca.* 4-5 due to the use of the acetate buffer stocks in place of a concentrated HCl solution. Inspection of the reactions after a 4 day resting period revealed crystals of the pure $\{\text{Mo}_{132}\}$ target had formed for reaction numbers 29 (cH) and 39 (dH). The small dark brown polyhedral crystals were confirmed as $\{\text{Mo}_{132}\}$ by unit cell checks and IR and visible absorbance spectroscopy.^[6c]

Compounds **4** and **5** were isolated from the same reaction screening array where the dithionite reducing agent was set at 10 mol% and the ratio of reduced molybdate : H₂SO₄ was varied across the scan. The original target for this discovery array scan was in fact compound **5**, the $\{\text{Mo}_{368}\}$ “lemon”,^[6d] as proof that even some of the most complex POM structures could be accessed using this screening methodology. However in addition to finding conditions that successfully crystallized this product (Fraction 28, cI), conditions which crystallized **4**, the $\{\text{Mo}_{102}\}$ Keplerate,^[9] directly from the reaction solution were also found (Fraction 29, cJ). (For reaction conditions and product analyses see supplementary).

After crystals of compounds **1** - **5** were obtained from each discovery array, the reaction numbers provided a direct link, or “coordinates”, to the flow rates used to generate the solutions from which the target compounds crystallized. The pumps could then be programmed to run at these rates in a repetitive fashion, collecting multiple batches of each of the desired solution compositions, thus directly scaling-up the production of each of the target products. Over the multiple batches of crystallizations collected for compounds **1-3** the yields of crystalline material obtained remained consistently high throughout each set of batches: Average yield of $\{\text{Mo}_{36}\}$ from repeated batches of conditions 36 (dF) = 78.7 ± 5.3% over 10 reactions, average yield of $\{\text{Mo}_{154}\}$ from repeated batches of conditions 25 (cE) = 39.9 ± 2.8% over 10 reactions, average yield of $\{\text{Mo}_{132}\}$ from repeated batches of conditions 29 (cI) = 49.4 ± 4.4 % over 10 reactions, all of which are consistent with the single batch procedures previously reported in the literature.^[6] (For individual batch yields see supplementary fig. S4 – S6).

To further demonstrate the general scope of this combined synthetic approach, the area of Single Molecule Magnets (SMMs) was subsequently targeted. The synthesis and physical analysis of SMMs is an area of intensive research within coordination chemistry due to the potential applications these

materials may have in information storage, molecular spintronics, quantum computing and magnetic refrigeration.^[10] However similar to POMs, this increased attention has not led to the development or use of new synthetic methods outwith standard bench-top batch procedures. A family of oxime-based manganese clusters, originally synthesised by Brechin *et al.*,^[7] were chosen as exemplary SMM targets for the multiple pump reactor setup. The physical setup of the pumps and tubing for the reactor system remained unchanged except the POM reagent set was replaced with those relevant to the SMM syntheses (Figure 5.). The reagent set chosen for the SMM syntheses consisted of reagent grade MeOH for dilution; 0.5 M $\text{Mn}(\text{ClO}_4)_2 \cdot 6\text{H}_2\text{O}$ in MeOH as the Mn source; 0.5 M Triethylamine (TEA) in MeOH as the base; and 0.25 M Ethyl Salicyloxime (Et-saoH₂) in MeOH, 1.5 M 4-*tert*-butylpyridine (tBuPy) in MeOH and 0.125 M Pivalic acid (Piv) in MeOH and 0.125 M 2-hydroxymethylpyridine (hmp) in MeOH as ligand sources.

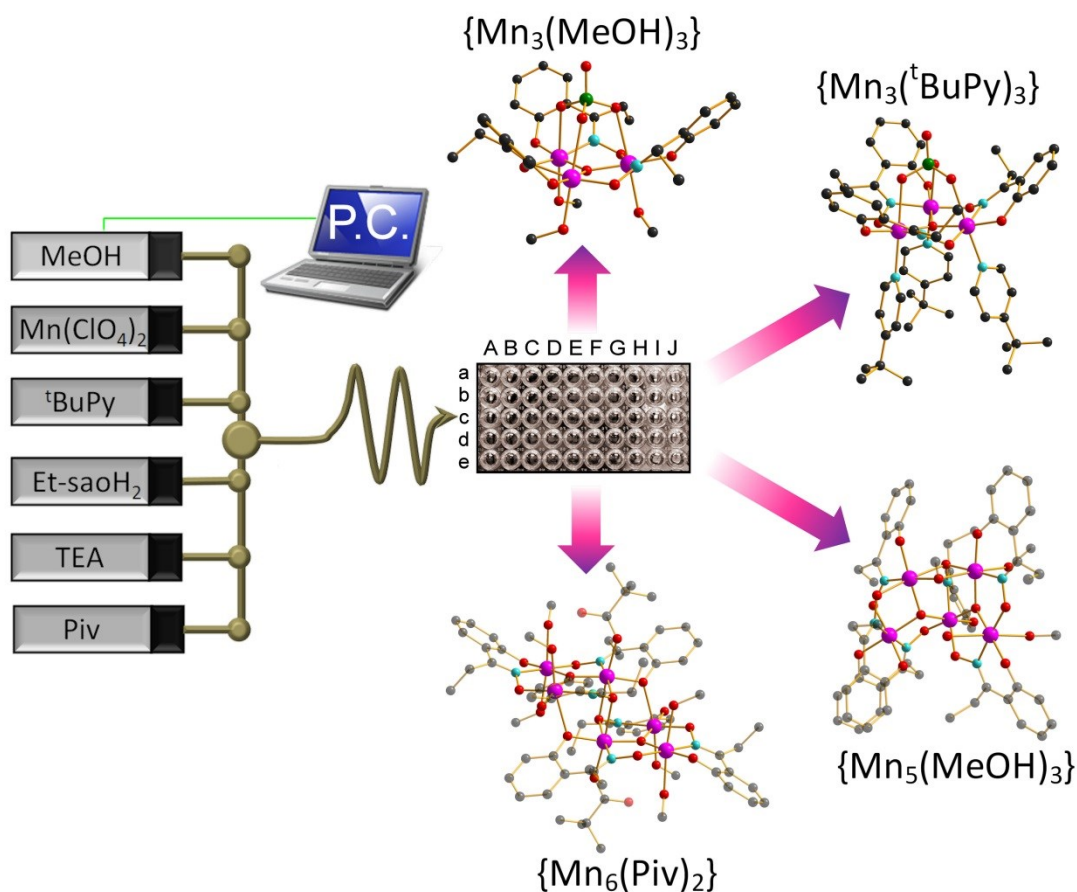


Figure 5. Schematic of the reagents and pump setup for the synthesis of the Mn Clusters. Cluster models are shown in their ball and stick representation with the colour scheme; Mn (magenta); Cl (green); N (light blue); O (red); C (grey): Hydrogen atoms are omitted for clarity.

To scan the reaction parameters surrounding the SMM compound **6**, $\text{Mn}_3\text{O}(\text{Et-sao})_3(\text{MeOH})_3(\text{ClO}_4)$, the starting point (reaction number 1, aA) was set at an initial dilution ratio of 8:2 (*i.e.* 80% MeOH and 20% reagent solutions by volume), the Mn:TEA ratio was set at a constant 1:1 by volume, and the Et-saoH₂ ligand was set at 0%. The Et-saoH₂ content with respect to Mn and TEA by volume was then increased to 90% in increments of 10% across the first row of reactions. The second row (row b) in the array began with the dilution ratio set to 6:4 and the Et-saoH₂ content reset to 0%. The ratio of Et-saoH₂ with respect to TEA and Mn then increased across each row of the array as the dilution factor decreased down the columns. Surprisingly, almost half of the fifty reactions in the array resulted in the formation of dark square/rectangular block crystals after resting for 4 – 5 days (characterised as compound **6** via unit cell checks and CHN elemental analysis). Due to the large number of successful crystallizations from the array, a yield map for the product was calculated based on the theoretical Mn content for each reaction (see Figure 6. and supplementary fig. S7).

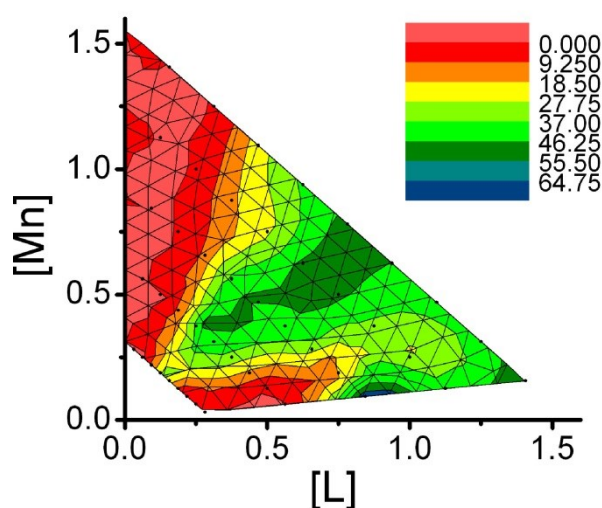


Figure 6. Contour plot of percentage yield as a function of manganese concentration, [Mn] and ligand concentration, [L] (mol L^{-1}). Trend shows optimum yields are obtained when [Mn] : [L] = 1:1 and are greater than 0.25 mol L^{-1} .

Inspection of the yield map graphic shows a general trend of product yield increasing with concentration but only whilst maintaining a molar ratio of 1:1. This is consistent with the product structure and with the conditions of the originally reported batch preparation.^[7a]

Similar discovery arrays were also set up for compound **7**, $\text{Mn}_3\text{O}(\text{Et-sao})_3(\text{tBuPy})_3(\text{ClO}_4)$, compound **8**, $\text{Mn}_5\text{O}_2(\text{Et-sao})_6(\text{MeO})(\text{H}_2\text{O})(\text{MeOH})_2$ and compound **9**, $\text{Mn}_6\text{O}_2(\text{Et-sao})_6(\text{Piv})_2(\text{MeOH})_6$. For compound **7**, the starting point (reaction number 1, aA) was set at an initial dilution ratio of 8:2 (*i.e.*

80% MeOH and 20% reagent solutions by volume), the Et-saoH₂:Mn:TEA ratio was set at a constant 2:1:1 by volume, and the tBuPy was set at 0%. Variation of the tBuPy and the dilution ratio subsequently led to the successful crystallization of compound **7** for a number of reactions in the array output. Compounds **8** and **9** were similarly obtained by variation of the other ligand sources with respect to the other reagents (see supplementary fig. S8 – S10).

Conclusions

In this report a new approach to molecular discovery of inorganic clusters and scale-up using automated adjustment of flow rates of precursor reagent solutions has been established. A selection of historically important polyoxomolybdate structures were synthesised as an initial proof of concept for the automated discovery of directly scalable reaction conditions. Application of the synthetic approach to obtain a small family of oxime-based Mn SMMs further demonstrated the scope for the possible expansion and use of this technology across the entire field of coordination chemistry. The ability to use such methods in cluster synthesis demonstrates the potential of this approach to revolutionise the way in which complex supermolecular and supramolecular systems are discovered and their syntheses optimised. Furthermore, the adoption of this technology in these areas would ideally place them to take full advantage of the advances in online solution based analytical techniques currently being developed for flow-based methodologies^[11] and could ultimately lead to a fully automated reaction setup capable of the discovery, optimisation and scale-up of syntheses for new inorganic clusters. In future work we will aim to expand this approach to other inorganic nanomaterial systems as well as complex organic reaction systems.

Methods

All chemicals were of analytical grade purchased from Sigma Aldrich, Fisher Scientific and Alfa Aesar chemical companies and used as supplied, without further purification. The standard stock solutions of each reagent were prepared using standard practices and volumetric glassware. All solutions were prepared with distilled deionised water and stored in plastic labware after preparation except reducing agent stocks which were freshly prepared (< 1hr) prior to each experiment run.

Pump System: The pump system set-up utilized between 3 and 8 programmable syringe pumps (C3000 model, Tricontinent Ltd, CA, USA) fitted with a 5 mL syringe and a 3-way solenoid valve, a LabVIEW™ based PC interface was used for controlling the pumps. FEP plastic tubing 1/8" OD was

cut to the specified lengths and connected using standard HPLC low pressure PTFE connectors and a PEEK manifold (Thames Restek, UK).

General procedure for the generation of reaction arrays: All reaction arrays were carried out using the following general procedures. Stock solutions of reagents were prepared and connected to the inlets for the assigned pumps. The connective tubing and pumps for all reagents were purged with the reagent solutions (3 mL) and the reactor tubing then flushed clean with fresh solvent (20 mL). The prewritten command scripts were then executed to initiate the pumping sequence (see supplementary .txt document). The fifty individual reaction batches were collected, manually changing test tubes at each programmed refill point. To take account of the reactor tubing volume, the first two reaction volumes collected were always discarded and two extra volumes of solvent were used to purge the reactor line at the end of each sequence. The samples collected were then left stationary for the specified resting period to allow crystallization of the products.

X-ray diffraction structure analysis and crystallographic data: **4:** $\text{H}_{716}\text{Mo}_{102}\text{Na}_{12}\text{O}_{688}\text{S}_{12}$, $M_r = 22176.2 \text{ g mol}^{-1}$; crystal size $0.09 \times 0.08 \times 0.04 \text{ mm}^3$; hexagonal system, space group, $R\bar{3}m$, $a = 32.2189(13)$, $c = 54.059(2) \text{ \AA}$, $V = 48598(4) \text{ \AA}^3$, $Z = 3$, $T = 150 \text{ K}$, $\rho_{\text{calcd}} = 2.273 \text{ g cm}^{-3}$, $\mu(\text{Mo K}\alpha) = 2.078 \text{ mm}^{-1}$, 113168 reflections measured, 10858 unique ($R_{\text{int}} = 0.177$) which were used in all calculations; structure solution and refinement were performed using WINGX^[12]. Final $R1 = 0.121$ and $wR2 = 0.389$ (all data). CSD-XXXXXX contains the supplementary crystallographic data for **4** (data available from CrysDATA@FIZ-Karlsruhe.de). **8:** $\text{C}_{60}\text{H}_{78}\text{Mn}_5\text{N}_6\text{O}_{21}$, $M_r = 1493.98 \text{ g mol}^{-1}$; crystal size $0.30 \times 0.10 \times 0.04 \text{ mm}^3$; Orthorhombic system, space group, $Pca2_1$, $a = 22.3613(3)$, $b = 15.2985(3)$, $c = 42.4185(7) \text{ \AA}$, $V = 14511.1(4) \text{ \AA}^3$, $Z = 8$, $T = 150 \text{ K}$, $\rho_{\text{calcd}} = 1.368 \text{ g cm}^{-3}$, $\mu(\text{Mo K}\alpha) = 0.917 \text{ mm}^{-1}$, 55250 reflections measured, 22958 unique ($R_{\text{int}} = 0.054$) which were used in all calculations; structure solution and refinement were performed using WINGX^[12]. Final $R1 = 0.065$ and $wR2 = 0.188$ (all data). CCDC XXXXXX contains the supplementary crystallographic data for **8**. These data can be obtained free of charge from The Cambridge Crystallographic Data Centre via www.ccdc.cam.ac.uk/data_request/cif

Elemental Analysis: Calcd. (found) for; compound **6**, $[\text{Mn}_3\text{O}(\text{C}_9\text{H}_9\text{NO}_2)_3(\text{OH}_2)_3(\text{ClO}_4)]$, C 39.36 (39.53), H 4.04 (4.01), N 5.10 (5.13); compound **7**, $[\text{Mn}_3\text{O}(\text{C}_9\text{H}_9\text{NO}_2)_3(\text{C}_9\text{H}_{13}\text{N})_3(\text{ClO}_4)]$, C 55.18 (55.19), H 5.66 (5.68), N 7.15 (7.19); compound **8**, $[\text{Mn}_5\text{O}_2(\text{C}_9\text{H}_9\text{NO}_2)_6(\text{CH}_3\text{O})(\text{H}_2\text{O})_3]$, C 48.19 (47.24), H 4.63 (4.24), N 6.13 (5.94); compound **9**, $[\text{Mn}_6\text{O}_2(\text{C}_9\text{H}_9\text{NO}_2)_6(\text{C}_5\text{H}_9\text{O}_2)_2(\text{H}_2\text{O})_6]$, C 46.56 (46.99), H 5.13 (4.62), N 5.09 (5.15).

References

- [1] Webb, D., Jamison, T. F., Continuous flow multi-step organic synthesis. *Chemical Science* **1**, 675 - 680 (2010).
- [2] Wegner, J., Ceylan, S., Kirschning, A., Ten key issues in modern flow chemistry. *Chem. Commun.* **47**, 4583 - 4592 (2011).
- [3] Abou-Hassan, A., Sandre, O., Cabuil, V., Microfluidics in Inorganic Chemistry *Angew. Chem., Int. Ed.* **49**, 6268 - 6286 (2010).
- [4] (a) Long, D.-L., Burkholder, E., Cronin, L., Polyoxometalate clusters, nanostructures and materials: From self assembly to designer materials and devices. *Chem. Soc. Rev.* **36**, 105 - 121 (2007). (b) Long, D.-L., Tsunashima, R., Cronin, L., Polyoxometalates: Building Blocks for Functional Nanoscale Systems. *Angew. Chem., Int. Ed.* **49**, 1736 - 1758. (2010). (c) Hill, C. L., Introduction: Polyoxometalates – multicomponent molecular vehicles to probe fundamental issues and practical problems. *Chem. Rev.* **98**, 1 - 2 (1998).
- [5] (a) Evangelisti, M., Brechin, E. K., Recipes for enhanced molecular cooling. *Dalton Trans.* **39**, 4672 - 4676 (2010). (b) Inglis, R., Milios, C. J., Jones, L. F., Piligkos, S., Brechin, E. K. Twisted molecular magnets. *Chem. Commun.* **48**, 181 - 190 (2012). (c) Kostakis, G. E., Hewitt, I. J., Ako, A. M., Mereacre, V., Powell, A. K. Magnetic coordination clusters and networks: synthesis and topological description. *Phil. Trans. R. Soc. A* **368**, 1509 - 1536 (2010). (d) Murrie, M., Cobalt(II) single-molecule magnets. *Chem. Soc. Rev.* **39**, 1986 - 1995 (2010). (e) Wang, X.-Y., Avendano, C., Dunbar, K. R. Molecular magnetic materials based on 4d and 5d transition metals. *Chem. Soc. Rev.* **40**, 3213 - 3238 (2011).
- [6] (a) Krebs, B., Stiller, S., Tytko, K. H., Mehmke, J., Structure and bonding in the high-molecular-weight isopolymolybdate ion, $(\text{Mo}_{36}\text{O}_{112}(\text{H}_2\text{O})_{16})^{8-}$ - the crystal structure of $\text{Na}_8(\text{Mo}_{36}\text{O}_{112}(\text{H}_2\text{O})_{16}) \cdot 58\text{H}_2\text{O}$. *Eur. J. Solid State Inorg. Chem.* **28**, 883 - 903 (1991). (b) Müller, A., Das, S. K., Fedin, V. P., Krickemeyer, E., Beugholt, C., Bögge, H., Schmidtman, M., Hauptfleisch, B., Rapid and simple isolation of the crystalline molybdenum-blue compounds with discrete and linked nanosized ring-shaped anions: $\text{Na}_{15}[\text{Mo}^{\text{VI}}_{126}\text{Mo}^{\text{V}}_{28}\text{O}_{462}\text{H}_{14}(\text{H}_2\text{O})_{70}]_{0.5}$ $[\text{Mo}^{\text{VI}}_{124}\text{Mo}^{\text{V}}_{28}\text{O}_{457}\text{H}_{14}(\text{H}_2\text{O})_{68}]_{0.5} \cdot \text{ca. } 400\text{H}_2\text{O}$ and $\text{Na}_{22}[\text{Mo}^{\text{VI}}_{118}\text{Mo}^{\text{V}}_{28}\text{O}_{442}\text{H}_{14}(\text{H}_2\text{O})_{58}] \cdot \text{ca. } 250\text{H}_2\text{O}$. *Z. Anorg. Allg. Chem.* **625**, 1187 - 1192 (1999). (c) Müller, A., Krickemeyer, E.; Bögge, H., Schmidtman, M., Peters, F., Organizational forms of matter: an inorganic super fullerene and keplerate based on molybdenum oxide. *Angew. Chem., Int. Ed.* **37**, 3359 - 3363 (1998). (d) Müller, A., Beckmann, E., Bögge, H., Schmidtman, M., Dress, A. Inorganic chemistry goes

- protein size: a Mo₃₆₈ nano-hedgehog initiating nanochemistry by symmetry breaking. *Angew. Chem., Int. Ed.*, **41**, 1162 - 1167 (2002).
- [7] (a) Inglis, R. et al. Enhancing SMM properties via axial distortion of Mn^{III}₃ clusters. *Chem. Commun.* **45**, 5924 - 5926 (2008). (b) Inglis, R. et al. Twisting, bending, stretching: strategies for making ferromagnetic [Mn^{III}₃] triangles. *Dalton Trans.* **42**, 9157 - 9168 (2009). (c) Inglis, R. et al. Attempting to understand (and control) the relationship between structure and magnetism in an extended family of Mn₆ single-molecule magnets. *Dalton Trans.* **18**, 3403-3412 (2009). (d) Kozoni, C., Siczek, M., Lis, T., Brechin, E. K., Milios, C. J., The first amino acid manganese cluster: a [Mn^{IV}₂Mn^{III}₃] dl-valine cage. *Dalton Trans.* **42**, 9117 - 9119 (2009).
- [8] (a) Müller, A. et al. [Mo₁₅₄(NO)₁₄O₄₂₀(OH)₂₈(H₂O)₇₀]^{(25±5)-}: A water-soluble big wheel with more than 700 atoms and a relative molecular mass of about 24000. *Angew. Chem., Int. Ed.* **34**, 2122-2124 (1995). (b) Müller, A., Meyer, J., Krickemeyer, E., Diemann, E., Molybdenum Blue: A 200 Year Old Mystery Unveiled. *Angew. Chem., Int. Ed.* **35**, 1206 - 1208 (1996).
- [9] (a) Müller, A. et al. Thirty electrons “trapped” in a spherical matrix: a molybdenum oxide-based nanostructured keplerate reduced by 36 electrons. *Angew. Chem., Int. Ed.* **39**, 1614 - 1616 (2000). (b) Müller, A., Krickemeyer, E., Bögge, H., Schmidtman, M., Botar, B., Talismanova, M. O. Drawing small cations into highly charged porous nanocontainers reveals “water” assembly and related interaction problems. *Angew. Chem., Int. Ed.* **42**, 2085 - 2090 (2003). (c) Henry, M., Bögge, H., Diemann, E., Müller, A., Chameleon water: assemblies confined in nanocapsules. *J. Mol. Liq.* **118**, 155 - 162 (2005).
- [10] (a) Bogani, L., Wernsdorfer, W., Molecular spintronics using single-molecule magnets. *Nat. Mater.* **7**, 179 - 186 (2008). (b) Evangelisti, M., Luis, F., de Jongh, L. J., Affronte, M., Magnetothermal properties of molecule-based materials. *J. Mater. Chem.* **16**, 2534 - 2549 (2006). (c) Zheng, Y.-Z., Evangelisti, M., Tuna, F., Winpenny, R. E. P., Co-Ln Mixed-metal phosphonate grids and cages as molecular magnetic refrigerants. *J. Am. Chem. Soc.* **134**, 1057 – 1065 (2012). (d) Leuenberger, M. N., Loss, D., Quantum computing in molecular magnets. *Nature*, **410**, 789 - 793 (2001). (e) Lehmann, J., Gaita-Arino, A., Coronado, E., Loss, D., Spin qubits with electrically gated polyoxometalate molecules. *Nat. Nano*, **2**, 312-317 (2007). (f) Karotsis, G. et al. [Mn^{III}₄Ln^{III}₄] Calix[4]arene clusters as enhanced magnetic coolers and molecular magnets. *J. Am. Chem. Soc.* **132**, 12983 - 12990 (2010).
- [11] (a) Lange, H., Carter, C. F., Hopkin, M. D., Burke, A., Goode, J. G., Baxendale, I. R., Ley, S. V., A breakthrough method for the accurate addition of reagents in multi-step segmented flow processing. *Chemical Science*, **2**, 765 - 769 (2011). (b) McMullen, J. P., Stone, M. T., Buchwald, S. L., Jensen, K. F., An integrated microreactor system for self-optimization of a heck reaction:

from micro- to mesoscale flow systems. *Angew. Chem., Int. Ed.*, **49**, 7076 - 7080 (2010). (c)
Parrott, A. J., Bourne, R. A., Akien, G. R., Irvine, D. J., Poliakoff, M., Self-optimizing continuous reactions in supercritical carbon dioxide. *Angew. Chem., Int. Ed.* **50**, 3788 - 3792 (2011). (d)
Rasheed, M., Wirth, T., Intelligent microflow: development of self-optimizing reaction systems. *Angew. Chem., Int. Ed.*, **50**, 357 - 358 (2011).

[12] Farrugia, L. J. *WinGX* suite for small-molecule single-crystal crystallography. *J. Appl. Cryst.*, **32**, 837 - 838 (1999).